A pulsed cathodic arc spacecraft propulsion system

2009 Plasma Sources Sci. Technol. 18 045005

(http://iopscience.iop.org/0963-0252/18/4/045005)

Plasma Sources Sci. Technol. **18** (2009) 045005 (8pp) doi:10.1088/0963-0252/18/4/045005

A pulsed cathodic arc spacecraft propulsion system

P R C Neumann, M M M Bilek, R N Tarrant and D R McKenzie

School of Physics, University of Sydney, NSW 2006 Australia

Received 8 October 2008, in final form 9 May 2009
Published 31 July 2009
Online at stacks.iop.org/PSST/18/045005

Abstract
We investigate the use of a centre-triggered cathodic arc as a spacecraft propulsion system that uses an inert solid as a source of plasma. The cathodic vacuum arc produces almost fully ionized plasma with a high exhaust velocity ($>10^4$ m s^{-1}), giving a specific impulse competitive with other plasma or ion thrusters. A centre trigger design is employed that enables efficient use of cathode material and a high pulse-to-pulse repeatability. We compare three anode geometries, two pulse current profiles and two pulse durations for their effects on impulse generation, energy and cathode material usage efficiency. Impulse measurement is achieved through the use of a free-swinging pendulum target constructed from a polymer material. Measurements show that impulse is accurately controlled by varying cathode current. The cylindrical anode gave the highest energy efficiency. Cathode usage is optimized by choosing a sawtooth current profile. There is no requirement for an exhaust charge neutralization system.

(Some figures in this article are in colour only in the electronic version)

1. Introduction

Solid fuel electric propulsion systems that use inert fuels and have no moving mechanical parts (such as valves and pressure regulators) are attractive for long-duration spaceflight applications, especially for station keeping and positioning. Pulsed vacuum arcs have been the subject of research for industrial application for decades, but have not been considered to be competitive with other spacecraft electric propulsion methods until relatively recently [1]. An application to micro-thrusters has been described [2]. They are attractive from a propulsion perspective due to the high drift velocity of the plasma plume [2], the high ionization fraction of the plasma [2] and because the plasma plume is quasi-neutral [2].

Various electric propulsion methods have developed sufficient technological maturity to be deployed in space, such as arcjets, resistojets, pulsed plasma thrusters (PPTs) and Hall effect thrusters [3]. An arcjet uses an arc to heat and expel a gas, while a PPT uses an arc to ablate a solid insulating material. These thrusters are distinct from a cathodic vacuum arc thruster in that they do not directly use the cathode material as the propellant. Each of these systems has a limitation of either a low exhaust velocity or a plasma exhaust that requires charge neutralization. A pulsed arc system has neither of these drawbacks. This paper aims to investigate the potential of a pulsed cathodic arc system as a spacecraft motor. We investigate the effect of pulse profile, duration, current magnitude and anode configuration on the magnitude of the impulse delivered and the energy efficiency of the system.

2. Design considerations

In a vacuum cathodic arc a discharge is struck between a solid conductive cathode and an anode. The arc current is carried by ablated cathode material, in the form of a plasma [4]. Some of this charged material includes ionized metal vapour, which is ejected normal to the cathode surface at velocities on the order of 1–2 $\times$ 10^4 m s^{-1} [5].

The discharge can be triggered in a variety of ways, including laser, mechanical and electrical triggering [6]. We chose an electrical triggering system because there are no moving parts and it avoids the complications associated with using high powered pulse lasers in space. Although the trigger can be located anywhere on the face of the cathode, we chose to use a centre-triggered system as it ensures a more even cathode erosion profile over the life of the cathode [7].

The arc spots move away from the trigger location and away from each other and erode the cathode along their trajectories [7, 8]. In centre-triggered systems, the arc spots

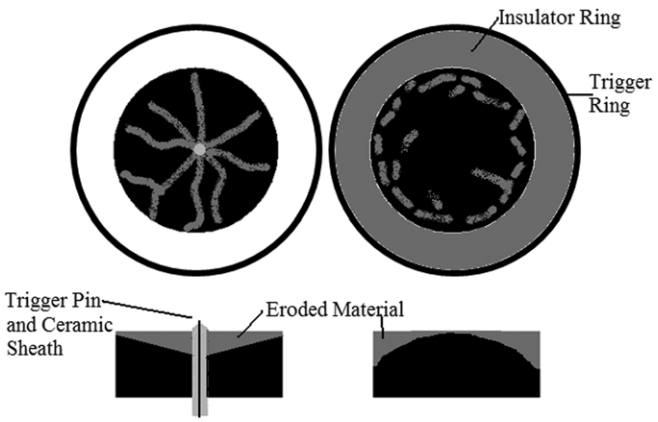

Figure 1. Centre-triggered (left) and edge-triggered (right) systems. Centre-triggered arc spots move radially to the edge in a dendritic pattern, excavating a conical pit, while edge-triggered arc spots run about the edge of the cathode [7]. In our case, the trigger pin is a 1 mm diameter tungsten wire encased in an alumina sheath of 3 mm external diameter.

migrate outwards to the edges in a dendritic pattern [8], whereas edge triggering causes the arc spots to move around the outer edge of the cathode [7]. Thus, the centre-triggered system will erode a star pattern into the face of the cathode, while the edge-triggered system will round off the edges of the cathode, as shown in figure 1. Work by Gan *et al* [7] has shown that forward directed plasma production diminishes after many pulses in edge-triggered systems, while it is maintained in a centre-triggered system.

Since plasma is ejected normal to the cathode surface, greater directionality of the plasma plume will result in more momentum transfer in the thrust direction and less momentum directed sideways. Thus, smaller angles of the cathode surface with respect to a flat plane will result in greater and more reproducible thrust [7]. Higher reproducibility is achieved by preventing the arc spots generated in the centre of the cathode face from running off onto the side of the cathode, which causes side-arcing to the anode or chamber walls. Side-arcing wastes cathode material (fuel) and lowers total momentum production, and can be prevented by cutting the arc power supply before the spots reach the edge of the cathode.

Operating in pulsed mode allows the use of high currents, leading to the creation of many arc spots, which evens out the stochastic nature of each spot source. Another advantage of high current pulsed arc systems is that the production of cathode debris, or 'macroparticles,' is minimized [13–15]. Macroparticles emerge with velocities much lower than that of the plasma plume (a few tens of metres per second), and so are wasting cathode material in that they contribute to cathode erosion, but do not contribute appreciably to thrust.

The charge environment of spacecraft can vary significantly in different orbits as the craft travels through different regions of space plasma [9, 10]. Plasma exhaust from electrical propulsion systems can alter the floating potential of the surrounding space plasma, altering the potential to which the spacecraft will be charged. Charging of the skin relative to internal components is undesirable as it can lead to damaging electrical breakdowns. This can be mitigated by connecting

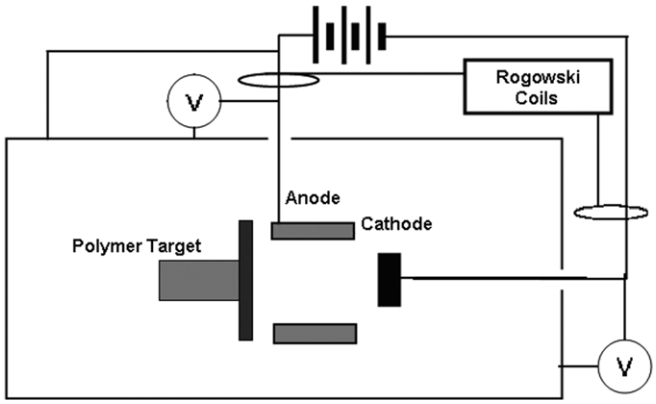

Figure 2. Schematic diagram of the system, employing a cylindrical anode. The polymer target is suspended as a pendulum and measures impulse delivered. V denotes a voltmeter.

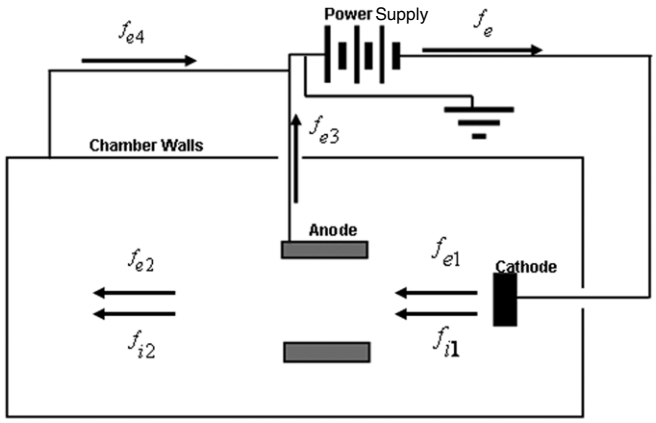

Figure 3. A circuit diagram of the arc system, showing particle fluences.

the anode to the spacecraft skin. In our test system the anode and vacuum chamber walls share a common ground as shown in figure 2.

Figure 3 shows a simplified circuit diagram with ion and electron fluences indicated. Where particle fluences are given as f, the subscript i denotes ion fluence and e denotes electron fluence. Conversion to currents is achieved by multiplying the fluences by the charge of the particles they represent, being $\bar{q}$ for the average ion charge state and e for the electronic charge. An application of Kirchoff's current law gives the following instantaneous equations:

$$ef_{\mathrm{e}} + \bar{q}_1 f_{\mathrm{i}1} = ef_{\mathrm{e}1}. \tag{1}$$

Equation (1) relates the currents flowing through the cathode, namely the electron current supplied by the power supply and the ion and electron currents leaving the cathode in the plasma.

$$ef_{\mathrm{e}1} + \bar{q}_2 f_{\mathrm{i}2} = ef_{\mathrm{e}3} + ef_{\mathrm{e}2} + \bar{q}_1 f_{\mathrm{i}1}. \tag{2}$$

Equation (2) describes the operation of the anode. There are input fluences from the plasma, as well as output plasma fluences from any plasma that exits the anode aperture. Whatever charge is collected by the anode is returned to the system's common earth. For high thrust production, it is clear that a large output ion fluence $f_{\mathrm{i}2}$ is desirable, and it follows

that f_{e2} must be of comparable order in order to maintain quasi-neutrality. However, for stable operation of the arc, there must be a sufficiently large anode fluence f_{e3}, but this limits the flux of electrons available to balance the ion flux in the quasi-neutral plasma ejected from the anode mouth. Thus, the input electron fluence, f_{e1} must be much larger than the output electron fluence, f_{e2}. In order to achieve this there must be a low impedance pathway from the cathode to the anode. If such a pathway does not exist, a high burning voltage combined with a low anode current is observed.

$$ef_e = ef_{e4} + ef_{e3}. \tag{3}$$

Equation (3) is the return node equation and shows that the sum of the return currents is equal to the cathode current.

$$ef_{e4} + \bar{q}_2 f_{i2} = ef_{e2} + I_{walls}(t). \tag{4}$$

Equation (4) describes the collection of ejected plasma by the chamber walls and its return to the main circuit. The circuit diagram is drawn to represent our laboratory system, but is equally applicable to a spacecraft by generalizing the chamber walls to include the spacecraft skin and the region of weakly ionized plasma in its vicinity. I_{walls} represents the charging current that flows to modify the potential of the spacecraft skin. The potential of the spacecraft skin will eventually reach equilibrium, at which I_{walls} integrates to zero over each cycle. Equation (4) is necessary to describe the current drawn from space plasma [9], as this can be large and depends on spacecraft orientation, velocity and orbital parameters.

Since the net ejected particle fluence from a cathodic arc is higher for electrons than ions [2, 4], the spacecraft will charge positively with respect to the local plasma potential, so that it will attract more electrons from space. The ejected ion fluence, f_{i2}, will not be attracted back to the surface of the spacecraft, thus eliminating the need for electron guns to neutralize the exhaust. This is in contrast to Hall effect thrusters, which require an electron gun to prevent the attraction of the ions back onto the spacecraft, because they would otherwise expel net positive charge.

3. Experiment

The experimental work was undertaken using the high current centre-triggered pulsed cathodic vacuum arc at the University of Sydney [5]. A schematic block diagram of the system is shown in figure 2. This figure, while not to scale, shows the sensors used in these experiments. The currents through the anode and cathode leads were measured using Rogowski coils whose signal was fed through integrators into a Tektronix TDS 2014 digital oscilloscope. Voltage probes were used to determine the cathode and anode running voltages, with these signals also being sent to a Tektronix TDS 2014 digital oscilloscope. The polymer target used to determine the impulse delivered by the system will be discussed later. Power was supplied to the system by means of a capacitor bank, whose pulse profile could be altered, by the addition of extra capacitors and inductors, between one of two forms, either a 'square' or a 'sawtooth' profile. The inclusion of an extra 15 mF capacitor in the circuit close to the cathode allowed a square current profile to be realized at the cathode face by inserting an extra fast-rising current pulse. The system generates an approximately sawtooth current profile if left unmodified. These two profiles are shown as figure 3.

Previous work by Ryves *et al* [11] has shown differences in arc spot migration in these two modes of operation, leading to changes in the wear patterns, as shown in figure 4. It has been found that sawtooth current profiles lead to more even cathode wear and greater cathode longevity.

The system, shown schematically in figure 2, uses centre-triggered cathodes surrounded by a concentric anode to create the plasma [5]. Three anode geometries; cylindrical, bell and plate, as shown in figure 5, were selected for testing.

The cylindrical anode had an internal diameter of 75 mm and was 80 mm long. The bell anode had a mouth diameter of 50 mm, a throat diameter of 100 mm and a total length of 90 mm. The plate anode was a rounded octagonal plate 1.5 mm thick, 130 mm across the diagonal measurements with a 62 mm circular hole in the centre. All anodes were made from copper, as was the water-jacketed cathode mount. All experiments used a 50 mm titanium cathode.

Two pulse durations of 400 and 500 μs were selected. The cathode current was varied by changing the charging voltage on the power supply capacitor bank.

4. Impulse measurement

Due to limitations imposed by the environment and powerful transient EM fields generated by the arc during its operation, electronic load cells to measure directly the impulse developed by the device were not feasible [12]. An indirect method was developed to measure the displacement of a pendulum caused by the impact of the plasma created by the arc. A lightweight polymer pendulum was suspended in the path of the plasma ~20 mm in front of the anode mouth, with a coarse periodic grating projecting normally from its rear face, as shown in figure 6.

This grating interrupts the path of a laser beam directed towards a photodiode. The photodiode voltage trace reveals peaks and troughs corresponding to interruptions of the laser beam by movement of the grating. Since the distance between the features on the grating is known to a high degree of accuracy, measuring the time between peaks and troughs on the photodiode trace allows the target velocity to be determined. Measuring the mass of the target allows the target momentum gain to be determined, which is related to the impulse delivered by the thruster.

Relating the impulse delivered to the pendulum to the total thrust developed by the motor relies on some assumptions. First, we assume all of the ejected material is received by and adheres to the pendulum. It was confirmed by observation of the profile of the deposition that the majority of the material of the plasma was received by the target. Second, we assume that the pendulum behaves as a simple pendulum. This was achieved by arranging the centre of the deposition to coincide with the centre of mass of the pendulum to avoid twisting.

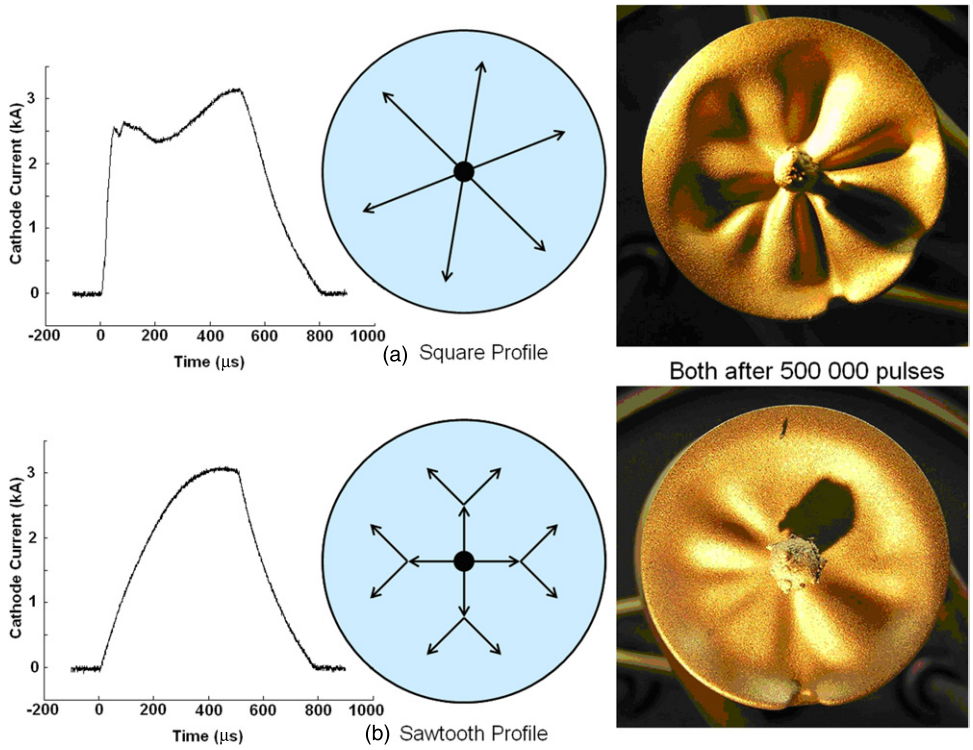

Figure 4. Comparison of representative arc currents, spot migration patterns and images of the cathodes after 500 000 pulses for (*a*) square current profiles and (*b*) sawtooth current profiles. Cathodes are 31 mm in diameter. Images provided with permission from Ryves *et al* [11].

It was also confirmed that the small angle approximation was justified by observing the displacement of the pendulum under plasma impact. The greatest displacement observed was ∼30 mm, which with a lever arm of approximately 160 mm, leads to an angular displacement of less than 10°, which is small enough to enable simple harmonic motion.

5. Sources of uncertainty in impulse measurement

5.1. Target mass

The target was weighed before and after the experiments, totaling 1635 pulses. A small net loss of mass of 0.1263 g was found, corresponding to 1.95% of the initial mass. This mass loss is due to outgassing from the polymer, and outweighs the mass gained by deposition from the plasma. The average of initial and final masses was used in the calculation, and the uncertainty in impulse arising from the mass uncertainty was ±1%.

5.2. Ion acceleration in the vicinity of the target

A plasma sheath forms around objects placed in a plasma. This sheath has an associated electric field, usually directed towards the object. This field will accelerate ions towards the object, increasing their momentum. However, there is no net momentum exchange with the target resulting from this acceleration in the sheath, since the target and ions form an action–reaction pair. Therefore there is no over-estimation of impulse due to sheath formation.

5.3. Pendulum displacement measurement

Sources of error in displacement measurement include friction, distortion of target and noise in the photodiode trace. Friction was minimized by hanging the target from fine, flexible copper wires. The target was observed to continue oscillating minutes after the application of an impulse. Thus, friction and wire stiffness were not significant sources of error in these measurements.

After the impact and plating of several hundred plasma pulses, the polymer sheet became distorted from its original planar shape. This resulted in a minor angle of grating plane dip and twist, which leads to uncertainty in the velocity measurement. In this case, the apparent separation between features developed by grating movement would be larger than the true separation by a factor of $\sec(t)\cos(d)$, where t is the angle of horizontal twist and d is the angle of grating plane dip. Twist angles result in greater apparent distance between features, while angles of dip (or rise) result in lower apparent distances between features. Angles of approximately 5° in either dip, twist or both were not exceeded, leading to less than 1% error from this source.

Noise in the photodiode trace is the most significant source of error in target velocity measurement. Several measurements were taken to reduce uncertainties. The total uncertainty is approximately 5%.

6. Results

Figure 7 shows the cathode and anode currents, and their difference (net ejected current, NEC, being the vector sum

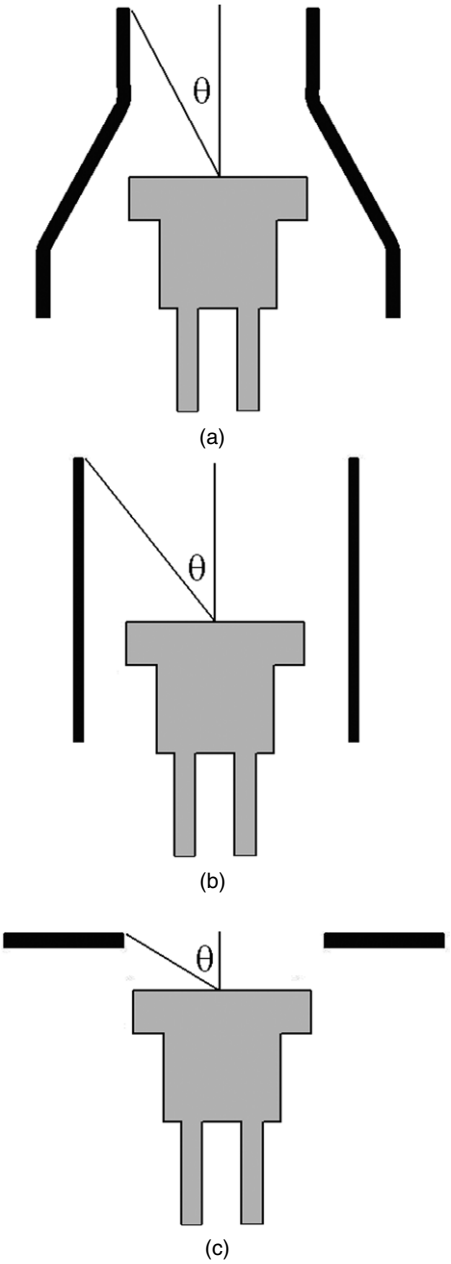

Figure 5. parts (*a*), (*b*) and (*c*) are side views of the anode–cathode assembly, being the bell, cylinder and plate anodes, respectively. In each sub-figure, the anode is black, while the cathode, cathode mount and cathode support pipes are grey.

of $\bar{q}\, f_{i2}$ and $e f_{e2}$) for a plate anode configuration and a square current pulse. The figure shows a low current at the beginning of the pulse, with a high burn voltage, until a transition is reached approximately 250 μs into the pulse. Equation (2) implies that if only a high impedance pathway from cathode to anode exists, low current will be drawn by the anode, thus fluence f_{e3} will be small and little plasma will form. Due to the high impedance of the overall circuit, the cathode current is low. This is not a desirable mode of operation for plasma generation.

After the transition at 250 μs, however, the arc settles into a more stable mode of operation. During this phase, the plasma produced by the arc spots can form a low impedance pathway

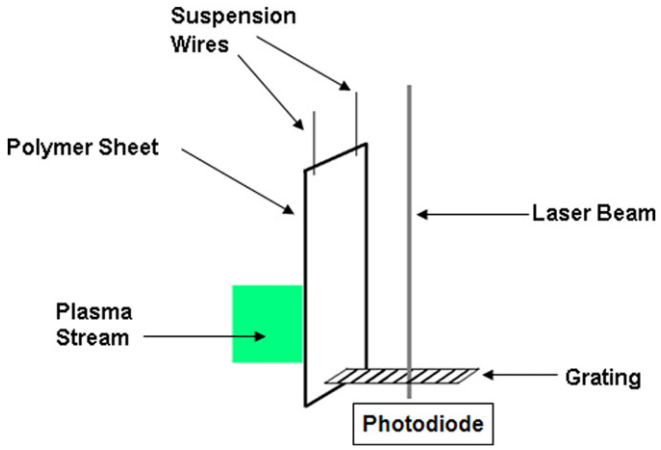

Figure 6. A schematic of the pendulum target, showing a plasma stream incident from left and a laser beam passing through a grating to measure the resulting displacement of the polymer sheet.

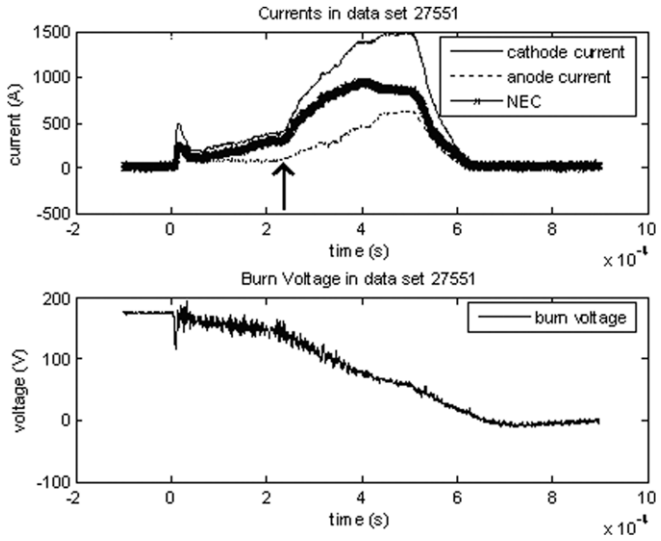

Figure 7. Plot of arc currents and burn voltage during a square pulse using the plate anode. Note the transition after 250 μs (arrowed), showing a jump in all currents and a fall in burn voltage. Prior to this transition the anode is not acting effectively. The high initial burning voltage implies a high initial impedance pathway.

to the anode, and so anode current significantly increases. This lower impedance is shown by the more rapid reduction in burn voltage after the transition. Since there is lower impedance, more current can flow at lower voltages, and so much more plasma is created. A large proportion of this plasma is directed forwards, through the mouth of the anode, towards the ballistic pendulum, delivering impulse to the pendulum.

Figure 8 shows the cathode and anode currents, and their difference for a bell anode configuration and a square current pulse profile. No transition is evident as the anode draws arc current from the beginning of the pulse. However, after 400 μs, the anode current begins to approach the cathode current while the NEC declines. This is evidence of side-arcing. For higher cathode currents, more arc spots are created. These arc spots spread more quickly due to increased repulsive forces between them and reach the edge of the cathode sooner. Thus, higher arc currents will lead to side arcing at the end of the pulse,

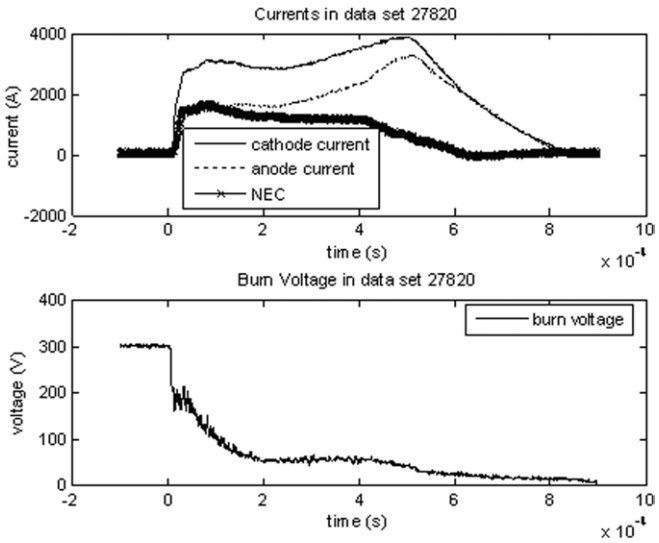

Figure 8. Plot of a well-behaved square profile arc using the bell anode. The increase in anode current towards the end of the pulse is indicative of side arcs. The initial high anode current shows that a portion of the plasma impacts the anode, rather than travel through the anode mouth.

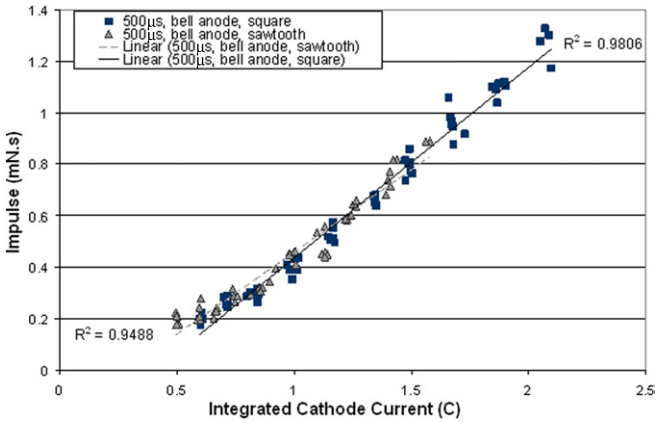

Figure 9. Impulse delivered as a function of integrated cathode current per pulse. Pulse current profile has no effect on momentum, which has a linear dependence on cathode current.

whilst the arc spots in lower current arcs do not have sufficient time to reach the edge of the cathode.

6.1. Effect of pulse profile on impulse delivered

Figure 9 shows a plot of impulse delivered against time-integrated cathode current for the two pulse profiles for 500 μs pulses using the bell anode. There is a strong linear correlation between the target impulse and the time-integrated cathode current per pulse, which is equivalent to the total charge transferred to the cathode over the pulse. The slopes for the two pulse profiles are very similar, which shows that the integrated charge is a good predictor of the total impulse delivered, independent of the pulse current profile, for a particular anode configuration. The results obtained for the plate and cylindrical anodes also showed no dependence on the pulse profile.

These results indicate that the shape of the pulse profile does not affect how much impulse is delivered for a given

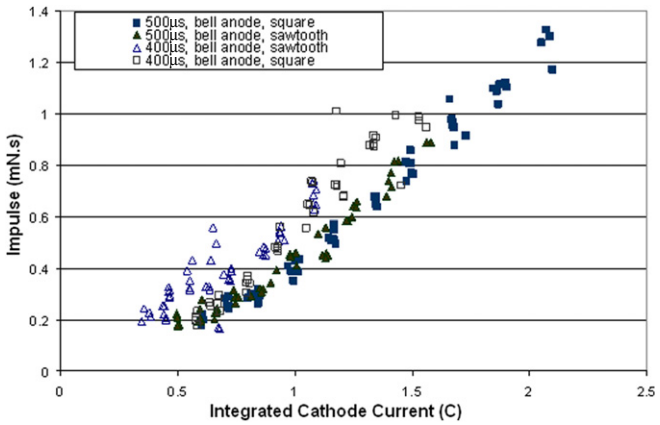

Figure 10. Comparison of impulse delivered as a function of integrated cathode current for pulse durations of 400 and 500 μs and two current profile shapes for the bell anode.

time-integrated cathode current. A similar independence of the pulse shape was observed when plotting the impulse against energy expenditure. This indicates that pulse shape is a free parameter when optimizing both for mass efficiency and energy efficiency. It has been shown by Ryves *et al* [11] that a sawtooth profile leads to more efficient cathode utilization. The sawtooth profile would therefore be more desirable for long-duration applications, or when cathode usage is the priority. However, square profiles can deliver more total impulse per pulse, and so would be more desirable for situations in which rapid changes in momentum were required.

6.2. Effect of pulse length

Figure 10 shows the impulse delivered as a function of integrated cathode current plots for two pulse durations and both pulse shapes. There is no effect of pulse shape on the impulse. There is, however, a strong dependence on pulse duration. An increase in pulse duration allows for more plasma to be generated, leading to more material being expelled from the cathode.

While more total impulse is delivered by longer pulses, it appears that the 400 μs pulses are more efficient. The 400 μs pulse curves show more impulse delivered for a given integrated cathode current. This is probably due to the increased prevalence of side arcing in long pulses, as the arc spots have sufficient time to reach the edge of the cathode, and arc sideways to the anode [7]. Therefore, the shorter duration pulses are more efficient, in that there is more momentum generated from a given quantity of material ejected from the cathode and energy consumed. This indicates that for different regimes, different pulse durations may be optimal, but the net result is a confirmation of the assertion that longer pulse durations deliver more impulse.

6.3. Effect of anode geometry on impulse as a function of input energy

Figure 11 shows the relation between the momentum delivered to the target and the input energy for the three different anode designs. The input energy is the integral over one pulse

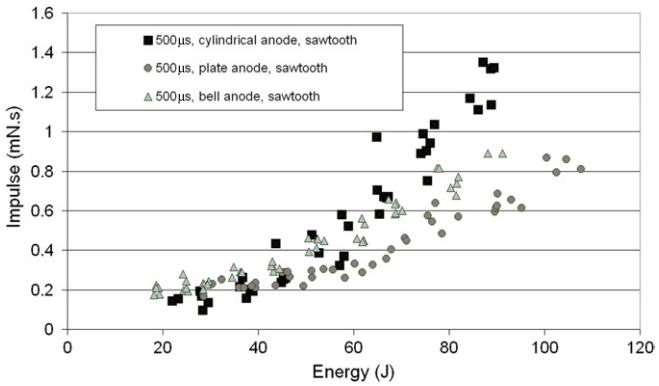

Figure 11. This figure shows that, for a given energy, the anodes can be ordering in decreasing effectiveness cylinder, bell, and plate, irrespective of pulse shape. The same effect is also seen for the shorter pulse length.

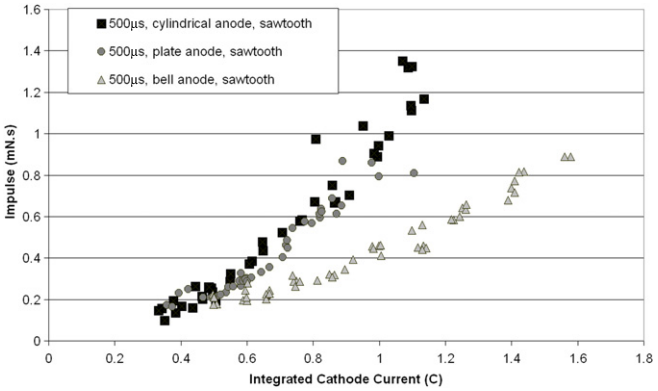

Figure 12. Impulse delivered as a function of integrated cathode current. Bell has inferior performance due to much lower solid angle subtended by the mouth of the bell anode, allowing less material out of the anode. Although the plate has a larger solid angle than the cylindrical anode, there is a cosine distribution, and for these large angles the additional effect is minimal.

of the product of the instantaneous cathode current and the instantaneous burn voltage. The bell anode has an almost linear relation between the impulse and the input energy, while the cylindrical and plate anodes show non-linear dependences. The plate anode shows some outlying points with a lower impulse. As discussed previously, early side-arcing can lead to a loss in impulse.

Comparing the anodes by energy expenditure leads to the conclusion that the plate anode is inferior by this metric, which is in agreement with the Kirchoff's Law explanation advanced earlier. The higher burn voltage early in the pulse leads to more dissipation of energy by the electrons, which carry the majority of the plasma current. Since the electrons do not contribute to the impulse delivered to the target, it follows that the ions gain less energy, and thus less momentum is delivered to the target. Once the plume can 'see' the anode, however, more plasma can be produced.

6.4. Effect of anode geometry on impulse as a function of integrated cathode current

The mass of material ablated from the cathode surface is approximately proportional to the integrated charge passing through the cathode [2]. The physics of the cathode spot ablation process does not depend on the current, since only the number of spots changes with current, not the characteristics of the spots. Thus an integration of the cathode current will allow qualitative comparisons between anode designs based on cathode usage rates. This integrated current is plotted for all anode configurations in figure 12. Note that the plate and cylinder anodes have similar performance envelopes, but that the bell anode supplies similar impulses at far higher cathode currents. This means that more material is ejected from the cathode, but does not reach the pendulum. Due to the smaller anode aperture angle, (shown as angle θ in figure 5) less of the ablated material can exit the anode. Thus, cathode material is consumed without contributing to the exhaust stream (and hence thrust). By the measure of integrated cathode current, the cylindrical anode and the plate anode are more efficient in their usage of cathode material than the bell anode.

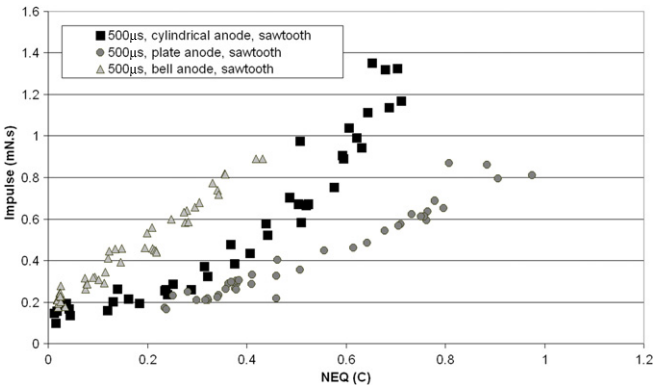

Figure 13. Impulse as a function of NEQ, showing that the anode with the smallest aperture solid angle gives the highest momentum per ion ejected through the anode, by restricting the expelled plasma to that which is directed most forwards.

6.5. Effect of anode geometry on impulse as a function of NEQ

While the integral of cathode current gives a measure of how much material is ejected from the surface of the cathode, another measure must be used to indicate how much material is expelled into the chamber. To do this, the integral of the NEC is used. This net ejected charge (NEQ) is plotted in figure 13 to allow comparison between the anode geometries based on mass-usage efficiencies. As figure 13 shows, the bell anode is more efficient by this metric, suggesting that the material is ejected more directionally.

This plot shows more evidence of the Kirchoff's Law explanation being correct, as greater impulse is generated for a given NEQ by the bell anode than by any other. This is due to the plasma being ejected more perpendicular to the anode mouth plane and thus towards the pendulum target. Comparison with the previous section shows that the charge expelled from the cathode to be very much more than that passing through the mouth of the bell anode, showing that most of the plasma impacts on the anode. However, the plate anode shows low impulse per unit charge ejected, showing that the

large anode aperture (angle θ in figure 5(*c*)) of the plate anode leads to suboptimal operation; while much of the plasma can escape, it is not well directed.

7. Discussion

The cylindrical anode geometry appears best in terms of impulse per unit energy expended and with respect to integrated cathode current. The cathode current is a measure of material ejected from the cathode, and so is a qualitative measure of fuel use rate. The bell anode plots are more repeatable than those of the other two configurations. There is also much less evidence for side-arcing in the data for the bell anode. Within the dimensions used in this work, it seems that a cylindrical geometry is superior based on these test results, but that the dimensions should be modified to minimize side-arcing.

It is known from the literature [2] that the plasma produced from arc discharges is distributed in a cosinusoidal pattern, with the bulk of the plume ejected normal to the cathode. Evidence for that is seen here, where little anode current is detected when using the plate anode, compared with the other anodes. Also, that the bell anode delivers superior impulse per unit charge ejected, but less impulse per unit cathode current. The area of the outlet of the bell anode is less than half the size of those of the plate or the cylinder. A bell anode with a larger outlet may possess the advantages of both the cylinder and bell configurations. The NEQ and integrated cathode current results show that plasma directionality is a design criterion, which justifies the design choice of a centre-triggered system.

Work by Ryves [11] shows that pulse current profile has a large effect on erosion patterns, with sawtooth profiles leading to more efficient cathode use. The work presented in this paper shows that the impulse delivered by both square and sawtooth current profiles have the same trend with regard to impulse per unit energy and impulse per unit charge. Based on this, a sawtooth profile is more effective in a long-duration application, as cathode material is used more effectively, as opposed to a square current profile, which is better for high impulse applications.

The high ion exit velocity directed normally to the cathode results in a high specific impulse, significantly higher than conventional electrical propulsion systems and is competitive with Hall effect thrusters such as the SNECMA Moteurs PPS-1350 [16]. If a sufficiently high duty cycle (∼50 Hz) is assumed for the pulsed arc system, the pulsed arc and the PPS-1350 deliver comparable momentum, but at different energy efficiencies. Our pulsed arc system, using a cylindrical anode, uses four times the energy of the PPS-1350 to generate comparable thrust. This deficiency needs to be addressed before a pulsed arc can be employed as a viable propulsion system. However, the pulsed arc system does not need a scarce and expensive gas such as xenon for a fuel, but can use cheap and abundant metals instead. Additionally, no gas tanks, pipes or pressure regulators are needed, as the fuel is stored as a stable solid, potentially leading to further savings in propulsion system mass.

8. Conclusion

The cathodic arc offers some key advantages as a solid fuel plasma thruster. The quasi-neutral plasma produced by the cathodic arc discharge avoids the need for plasma exhaust neutralization. We conclude that, of the three anode designs tested, the cylindrical anode is superior in terms of cathode usage efficiency, energy efficiency and total impulse developed. In terms of controllability and repeatability, the bell anode is superior. The plate anode does not appear to be a viable configuration. While the current profile does not affect the system efficiency, a sawtooth profile demonstrates the most effective cathode utilization. Longer pulse durations deliver greater impulse, whereas shorter pulse durations are more efficient in energy and material usage due to the prevalence of side arcing at the end of long pulses. The centre trigger design gives reliable and reproducible plasma pulses without change in the impulse as the cathode is eroded. The impulse per pulse is accurately predictable from the cathode current, and this would be useful to any spacecraft pilot wishing to accurately position their spacecraft.

References

[1] Anders A *et al* 2002 *Rev. Sci. Instrum.* **73** 925–7
[2] Keidar M *et al* 2005 *Plasma Sources Sci. Technol.* **14** 661–9
[3] Larson W and Wertz J (ed) 2004 *Space Mission Analysis and Design* 3rd edn (El Segundo, CA: Microcosm Press)
[4] Brown I and Oks E 1997 *IEEE Trans. Plasma Sci.* **25** 1222–8
[5] Oates T H W, Pigott J, McKenzie D R and Bilek M M M 2003 *Rev. Sci. Instrum.* **74** 4750–4
[6] Gilmour A and Lockwood D 1972 *Proc. IEEE* **60** 977–91
[7] Gan B K, Bilek M M M, McKenzie D R, Swift P D and McCredie G 2003 *Plasma Sources Sci. Technol.* **12** 508–12
[8] Anders A 2005 *IEEE Trans. Plasma Sci.* **33** 1456–64
[9] Ferguson D *et al* 2006 *IEEE Trans. Plasma Sci.* **34** 1948–58
[10] Tajmar M 2002 *J. Spacecr. Rockets* **39** 886–93
[11] Ryves L, McKenzie D R and Bilek M M M 2009 *IEEE Trans. Plasma Sci.* **37** 365–8
[12] Cubbin E A, Ziemer J K, Choueiri E Y and Jahn R G 1997 *Rev. Sci. Instrum.* **68** 2339–44
[13] Anders A, Oks E and Yushkov G 2007 *J. Appl. Phys.* **102** 043303
[14] Yushkov G and Anders A 2008 *Appl. Phys. Lett.* **92** 041502
[15] Anders A and Yushkov 2007 *Appl. Phys. Lett.* **91** 091502
[16] Kugelberg *et al* 2004 *Acta Astronaut.* **55** 121–30